Chemistry & Biology
Article

Specificity Analysis-Based Identification of New Methylation Targets of the SET7/9 Protein Lysine Methyltransferase

Arunkumar Dhayalan,[1,2,3] Srikanth Kudithipudi,[1,2] Philipp Rathert,[1,2,4] and Albert Jeltsch[1,*]
[1]Biochemistry Laboratory, School of Engineering and Science, Jacobs University Bremen, Campus Ring 1, 28759 Bremen, Germany
[2]These authors contributed equally to this work
[3]Present address: Department of Biotechnology, Pondicherry University, Puducherry 605014, India
[4]Present address: Cellzome AG, Meyerhofstrasse 1, 69117 Heidelberg, Germany
*Correspondence: a.jeltsch@jacobs-university.de
DOI 10.1016/j.chembiol.2010.11.014

SUMMARY

We applied peptide array methylation to determine an optimized target sequence for the SET7/9 (KMT7) protein lysine methyltransferase. Based on this, we identified 91 new peptide substrates from human proteins, many of them better than known substrates. We confirmed methylation of corresponding protein domains in vitro and in vivo with a high success rate for strongly methylated peptides and showed methylation of nine nonhistone proteins (AKA6, CENPC1, MeCP2, MINT, PPARBP, ZDH8, Cullin1, IRF1, and [weakly] TTK) and of H2A and H2B, which more than doubles the number of known SET7/9 targets. SET7/9 is inhibited by phosphorylation of histone and nonhistone substrate proteins. One lysine in the MINT protein is dimethylated in vitro and in vivo demonstrating that the product pattern created by SET7/9 depends on the amino acid sequence context of the target site.

INTRODUCTION

SET7/9 (KMT7) is a protein lysine methyltransferase (PKMT) that had been initially identified as a histone lysine methyltransferase which generates monomethylation at histone 3 lysine 4 (Wang et al., 2001; Xiao et al., 2003). The function of SET7/9 is not clear: on one hand, it plays a role in regulating euchromatic gene expression through H3K4 methylation (Brasacchio et al., 2009; Chakrabarti et al., 2003; Deering et al., 2009; Evans-Molina et al., 2009; Subramanian et al., 2008); on the other hand, it was shown that SET7/9 exhibits very weak activity on nucleosomal substrates (Wang et al., 2001), suggesting that the main function of SET7/9 is nonhistone protein methylation. Indeed, SET7/9 methylates several nonhistone proteins such as Dnmt1, p53, TAF10, estrogen receptor α, pRb, p65, and Tat protein of HIV1 (Chuikov et al., 2004; Couture et al., 2006; Ea and Baltimore, 2009; Kouskouti et al., 2004; Kurash et al., 2008; Munro et al., 2010; Pagans et al., 2010; Subramanian et al., 2008; Wang et al., 2009). Different functions were attributed to the protein methylation mediated by SET7/9. For example, methylation of Dnmt1 by SET7/9 reduces its stability (Wang et al., 2009), whereas methylation of p53 and estrogen receptor α (ER) leads to their activation and stabilization (Chuikov et al., 2004; Kurash et al., 2008; Subramanian et al., 2008). Methylation of TAF10 by SET7/9 increases the affinity of TAF10 for RNA polymerase II and thereby helps in the formation of the preinitiation complex (Kouskouti et al., 2004).

The methylation activity of SET7/9 toward different substrates suggests a relaxed specificity of the enzyme. Crystal structures of peptides from histone H3, p53, and TAF10 bound to SET7/9 indeed revealed a considerable plasticity in its peptide interaction (see Table S1 available online) (Chuikov et al., 2004; Couture et al., 2006; Subramanian et al., 2008; Xiao et al., 2003). From the crystal structures, it had been proposed that SET7/9 mainly recognizes the sequence motif [KR] [STA] K (in which the methylation site is underlined) in the target peptide (Couture et al., 2006). However, this motif is based on only very few known targets, which often were identified by similarity to each other and to the original H3K4 site. Here, we have determined the specificity profile of SET7/9 in a stepwise iterative approach by methylating a series of peptide arrays, which altogether comprised more than 1200 different peptides. By using the derived specificity profile of SET7/9, we identified more than 90 new nonhistone target peptides and also show strong methylation of H2A and H2B tails. SET7/9 methylated many of the new nonhistone target peptides much stronger than its known targets. We investigated the methylation of 12 new target proteins and demonstrated that SET7/9 methylates 9 proteins in vitro and 5 proteins in vivo. We have also shown that the product spectrum of SET7/9 depends on the nature of the substrate and that dimethylation is produced with a better substrate. In addition, we investigated the influence of modifications at the H3 peptide on enzyme activity in an unbiased approach and show that phosphorylation of histone and nonhistone substrates inhibit methylation by SET7/9.

RESULTS

Specificity Profile of SET7/9

To analyze the substrate specificity of SET7/9, we prepared histone H3 tail (1-21) peptide arrays on functionalized cellulose membranes by SPOT peptide synthesis (Frank, 2002; Reineke

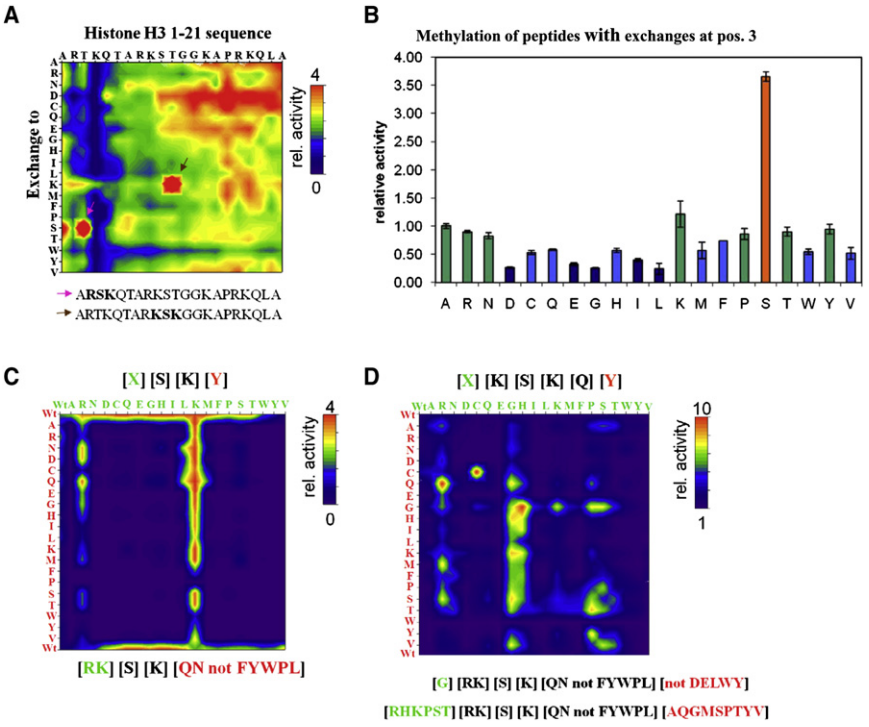

Figure 1. Specificity Analysis of Human SET7/9

(A) On the H3 tail 1-21 peptide each residue was exchanged against all 20 natural amino acid residues and the relative methylation by SET7/9 analyzed. Data are averaged numbers from three independent experiments. Methylation activities were normalized relative to methylation activity of SET7/9 on the natural H3 peptide.

(B) Relative methylation activity of SET7/9 on H3 tail peptides when T3 is exchanged with all other amino acids. The coloring scheme is based on relative activity (>1.2 orange, 1.2–0.8 green, 0.8–0.5 light blue, and <0.5 dark blue). Error bars represent standard deviations of three independent experiments.

(C) Two site randomization array where the K9 and G12 residues (−2 and +1 position) were exchanged against all 20 natural amino acid residues on the modified H3 T11K tail backbone (which is methylated at K11). Methylation activities were normalized relative to the methylation activity of SET7/9 on wild-type H3 peptide.

(D) Two site randomization array where the R8 and G13 residues (−3 and +2 positions) were exchanged against all 20 natural amino acid residues on the modified H3 T11K G12Q tail (with central KSKQ sequence with target K underlined). The raw data for this figure are provided in Table S4. See also Figure S1 and Table S1.

et al., 2001). In these arrays, each residue of the H3 tail was exchanged against all other 20 natural amino acids. The membranes containing the peptide arrays were incubated with purified SET7/9 enzyme in the presence of radioactively labeled S-adenosyl-L-methionine (AdoMet) and the transfer of the methyl group to the peptides on the membrane was detected by autoradiography. As expected, an exchange of the target lysine K4 of the H3 tail sequence with any other amino acid led to the complete loss of enzyme activity (Figure 1A). Specific sequence readout by SET7/9 was observed in the region between A1 and T6. However, we identified three spots, which were methylated much stronger by SET7/9 than the natural H3 1-21 peptide (Figure 1A). This effect was reproducible in different experiments using independently synthesized peptide arrays as substrates. One of these high activity peptides corresponded to H3 tail peptide in which T3 is exchanged with serine and the second one corresponded to the H3 T11K variant. The common feature of these two spots is the generation of a [KR] S K motif that is not present in the natural H3 tail sequence. In the first case, the T3S exchange places the K4 into an RSK context and in the second case the T11K exchange created a new KSK site with the new K11 as target. A third spot with increased activity is the A1S variant that can be understood in the light of data presented below.

A comparison of the methylation observed at all peptides in which T3 was exchanged (this residue corresponds to the −1 position, if the target lysine is considered position 0) showed that many residues are tolerated at this place (Figure 1B), but only S led to an increase in activity. With A, R, N, K, P, and Y, we observed activity similar (±20%) to T which is originally present at this place. Only D, E, G, I, and L led to a >50% reduction of activity.

The preference for [KR] S K motifs suggested that the real specificity of SET7/9 differs from the H3 template, stimulating us trying to identify an ''optimized'' target sequence. To this end, we have kept the SK motif as a main recognition motif in the H3 tail T11K sequence context (which gets methylated at the newly introduced K11) and exchanged the −2 position and +1 position against all other amino acids to cover all possible combinations of −2 and +1 residues. The highest activity was observed when R or K was introduced at the −2 position and Q or N was substituted at the +1 position. The enzyme showed moderate activity when the +1 position was substituted with all amino acids except F, Y, W, P, or L (Figure 1C). This result is summed up by the following motif:

[K > R] [S > KYARTPN] K [QN > other aa but not FYWPL]

Based on these results, we further extended the substrate specificity profile by keeping KSKQ as main recognition motif and exchanged the −3 and +2 positions with all other amino acids. The strongest activity of SET7/9 was observed when G is placed at the −3 position and moderate activity was also seen with R, H, K, P, S, or T at this position (Figure 1D). For position +2 the main result was that D, E, L, W, or Y inhibit methylation. By combining all the results from the different peptide array experiments, we derived two specificity profiles for the SET7/9 enzyme as:

G [K > R] [S > KYARTPN] K [QN > other aa but not FYWPL] [not DELWY] or

[RHKPST] [K > R] [S > KYARTPN] K [QN > other aa but not FYWPL] [AQGMSPTYV]

which may be combined as: [GRHKPST] [K > R] [S > KYARTPN] K [QN] [AQGMSPTYV]

This result includes the published specificity profile (Couture et al., 2006), but it shows important expansions and some

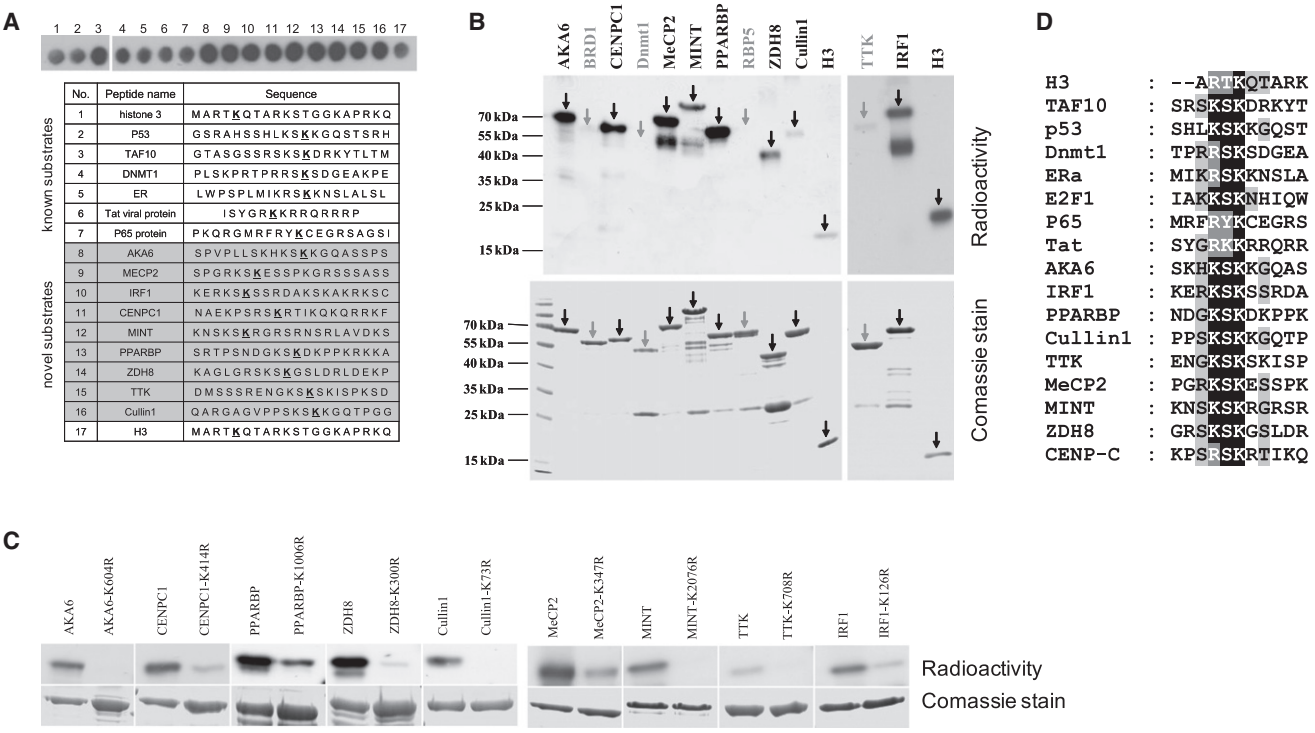

Figure 2. In Vitro Methylation of New Substrate Peptides and Proteins

(A) Comparison of the peptide methylation activity of SET7/9 on several known and newly identified substrates (the complete list of peptide substrates and methylation activities is available in Figure S2).

(B) Detection of protein methylation by transfer of radioactively labeled methyl groups. Purified GST-tagged protein domains were incubated with SET7/9 in the presence of radioactively labeled [methyl-3H]-AdoMet and separated on an SDS polyacrylamide gel, and the methylation of the target proteins was analyzed by autoradiography. As a control, methylation of histone H3 is shown. Methylated proteins are labeled in black color, not (or only very little) methylated proteins in gray.

(C) Identification of the modified lysine. The wild-type target proteins and the mutant proteins in which the target lysine residue was exchanged by arginine were methylated by SET7/9 using radioactive AdoMet.

(D) Alignment of some known and novel SET7/9 targets. The shading represents the agreement with the specificity profile.

See also Figure S3.

changes in detail. The clear preference for S over A at position −3 explains the high methylation of the H3 tail A1S variant mentioned before (Figure 1A).

Interestingly, the enzyme also showed high activity when cysteine was introduced simultaneously at the −3 and +2 positions (Figure 1D). This observation fits with the reported cocrystal structures of SET7/9 together with H3 peptide because the cysteines at positions −3 and +2 are located in a Cα distance of 5.5 Å (Figure S1). In the complex the target peptide forms a loop that could be covalently connected if the two cysteine residues form a disulfide bond. Thereby, the loop will be stabilized, which could explain better methylation by SET7/9.

SET/9 Methylates New Nonhistone target Peptides In Vitro

As described above, the sequence preferences of SET7/9 do not fully match the H3 peptide and some of the already identified nonhistone targets. Therefore, we were interested to investigate if the methylation of identified SET7/9 substrates agrees with our findings. We synthesized peptides corresponding to H3, p53, TAF10, DNMT1, ER, TAT, and p65 and investigated their methylation by SET7/9 and observed that TAF10 is the best substrate among them (Figure 2A; Figure S2). Next, we wanted to identify additional nonhistone substrates of SET7/9. To this end, a Scansite search (http://scansite.mit.edu/) was conducted using our SET7/9 specificity profiles which retrieved more than 400 human proteins containing potential target sites. Out of these, 118 proteins with known or predicted nuclear localization were selected for further analysis. In total, we have synthesized 133 peptides (derived from the 118 proteins) in duplicates and tested for methylation by SET7/9 on cellulose membranes (Figure 2A; Figure S2). It was observed that 44 peptides got strongly methylated, 47 peptides got weakly methylated and 42 peptides were not methylated by SET7/9. Since methylation of several substrates is performed in competition on the SPOT membranes, the methylation levels of different peptide spots correspond to k_{cat}/K_D values, which is a well-established measure of enzyme specificity (see Supplemental Information S1 in Rathert et al., 2008b). Hence, we conclude that the new peptides were methylated stronger than most of the previously known SET7/9 targets when presented on cellulose surface. We confirmed the stronger methylation of the MINT peptide than H3 peptide in solution as an example (see below).

The methylation levels of the different peptides showed a clear correlation with the net charge of the peptide, with positive charge increasing the methylation activity (Figure S3A). This result is in agreement with the observation that the substrate binding pocket of SET7/9 is flanked by many acidic residues (Figure S3B). The preference for positively charged substrates may also explain the weak methylation of H3 on nucleosome substrates (Wang et al., 2001) where the charge of the H3 tail is compensated by the bound DNA. A close inspection of the activities observed with the tested peptides suggests that the presence of the KSK motif embedded in a context of basic amino acid residues appears to be the most important parameter for SET7/9 activity.

SET/9 Methylates New Nonhistone target Proteins In Vitro

The peptide methylation assay is taking place on peptides bound to hydrated cellulose fibers which might influence reaction kinetics. Furthermore, the newly identified peptide substrates may not be accessible in the context of the target proteins. Therefore, it was important to investigate if nonhistone substrates were also methylated at the protein level. Fourteen target peptides were selected based on their high methylation and the corresponding protein domains cloned into a GST expression vector. The candidate nonhistone target protein domains were overexpressed and purified by affinity chromatography (Figure 2B). Out of the 14 target candidate protein domains, 12 got expressed well and could be purified. The protein domains from PRP4 and CRKRS failed in expression. The methylation of the purified proteins by SET7/9 was analyzed by incubating the protein domains with SET7/9 enzyme in a reaction buffer containing radioactively labeled AdoMet. The substrate protein domains were separated from radioactive cofactor and enzyme by SDS-PAGE. The methylation activity of SET7/9 on these protein domains was analyzed by measuring the transfer of radioactive methyl groups to the protein domains by autoradiography. Out of the 12 target protein domains, 9 were methylated by SET7/9, viz. AKA6, CENPC1, MeCP2, MINT, PPARBP, ZDH8, Cullin1, IRF1, and (weakly) TTK (Figure 2B). We have also included recombinant histone 3 as a positive control showing that many of the new nonhistone target domains were methylated by SET7/9 more efficiently than histone 3. The high yield of successful prediction of peptide and protein targets demonstrates the power of our peptide array-based specificity profile approach.

Site-directed mutagenesis was performed in the target protein domains to determine which lysine is methylated by SET7/9. To this end, the putative target lysines identified on the basis of the specificity profile of SET7/9 were exchanged to arginine. The mutated proteins were expressed and analyzed for methylation by SET7/9 (Figure 2C). SET7/9 showed no or strongly reduced activity on all mutant proteins confirming that they were methylated at the expected target lysine as predicted by the specificity profile of the SET7/9. In case of MeCP2, PPARBP, and IRF1, weak methylation was seen even after mutation of the predicted target lysine suggesting the presence of a second (weaker) methylation site in addition to the predicted target lysine. However, from the comparison of the intensities it is clear that our predicted target lysine is the primary target for SET7/9 in all three of these proteins (Figure 2C). Methylation of most target lysine residues was also confirmed by mass spectrometry (data not shown).

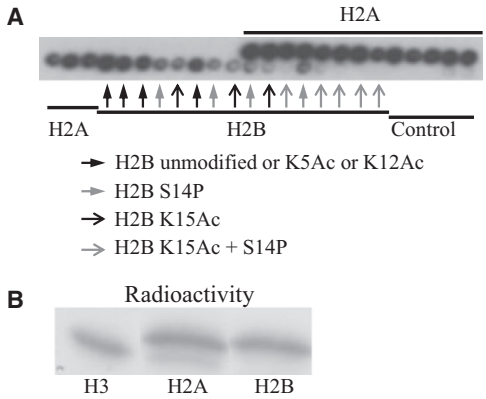

Figure 3. SET7/9 Activity on H2A and H2B N-Terminal Tails

(A) Methylation of H2A and H2B peptides containing different combinations of PTMs by SET7/9 (Table S3).

(B) Methylation of recombinant H3, H2A and H2B proteins. The histone proteins were incubated with SET7/9 in the presence of radioactively labeled [methyl-3H]-AdoMet and separated on an SDS polyacrylamide gel. The methylation of the target proteins was analyzed by autoradiography.

SET7/9 Methylates H2A and H2B Tails

It was recently shown that NSD2 methylates histone 4 in addition to the originally identified histone 3 target (Li et al., 2009). Similarly, G9a and GLP methylate histone H1 in addition to the initially identified histone 3 target (Rathert et al., 2008a; Weiss et al., 2010). However, the methyltransferase activity of SET7/9 toward other histone tails has not yet thoroughly studied. To this end, we methylated a histone tail peptide array with SET7/9. While only weak methylation was observed on the H4 tail (data not shown) strong methylation occurred on H2A and H2B (Figure 3A). Recombinant full-length H2A and H2B were also methylated by SET7/9 and their methylation efficiency is comparable with H3 methylation (Figure 3B).

Strong methylation of both H2A and H2B is not unexpected, since both are very basic (H2A: SGRGKQGGKARAKAKSRSS, net charge +7; H2B: PDPAKSAPAPKKGSKKAVT, net charge +4). The results with the peptide array suggest that SET7/9 methylates multiple lysines on H2A tail, since the acetylation of one or more lysine in these tails could not inhibit the SET7/9 activity (Figure 3A). This conclusion was confirmed by methylation studies with H2A tail variants in which all lysine residues were individually exchanged by alanine (data not shown). Multiple methylation sites in H2A are in agreement with having several lysine residues in H2A which are in a sequence context favorable for methylation, viz. K5 (R G K), K13 (R A K) and K15 (K A K). In contrast, K15 is the primary target lysine on H2B, since the acetylation of K15 blocks most of the SET7/9 activity while acetylation of other lysines (K5 and K12) had little influence (Figure 3A). Having K at position +1 and S at position −1, the sequence context of K15 of H2B fits to the specificity profile of SET7/9.

SET/9 Methylates New Nonhistone Targets In Vivo

The methylation of the nine new nonhistone protein domains was analyzed in human HEK293 cells by coexpression of the SET7/9

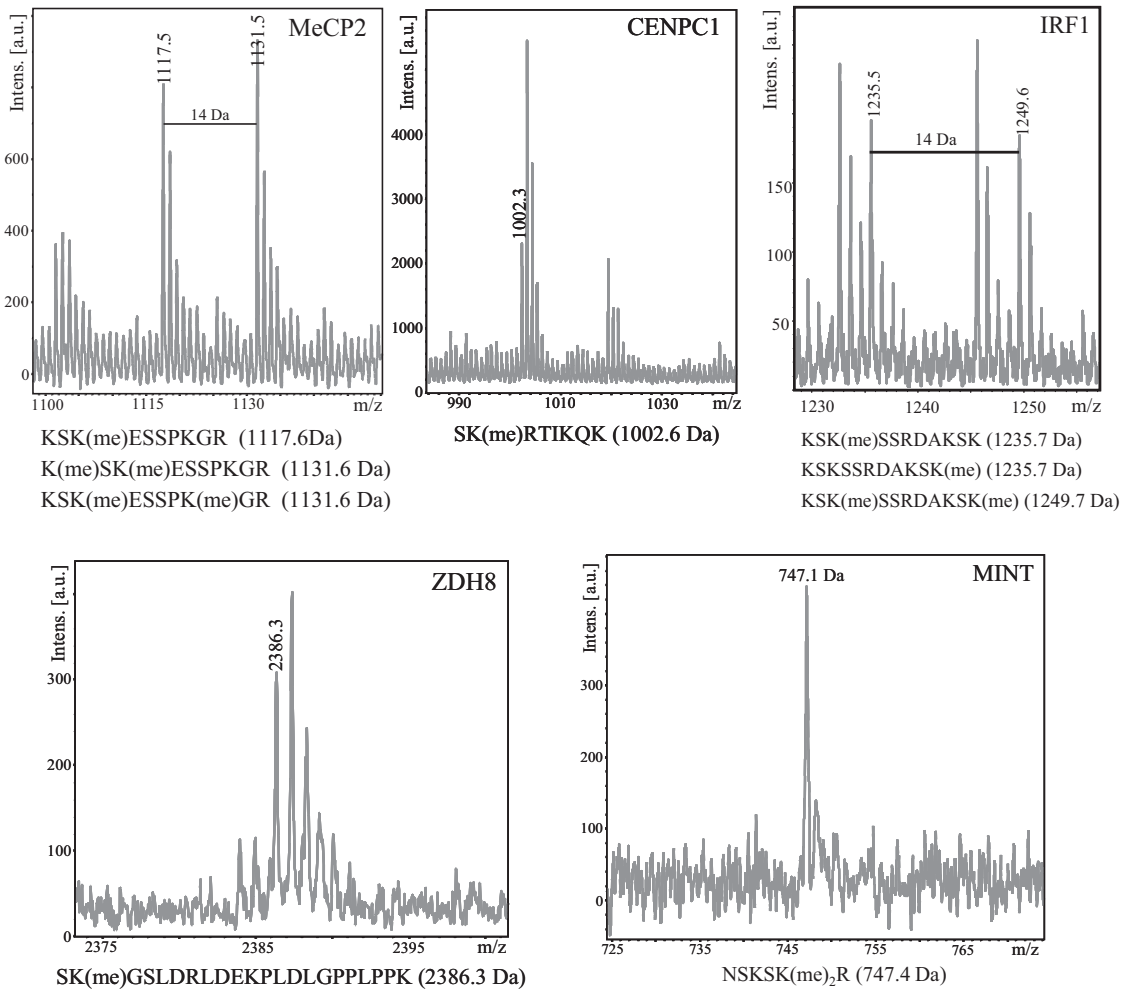

Figure 4. In Vivo Methylation of New Nonhistone Target Proteins by SET7/9

YFP-tagged target proteins were transiently expressed together with SET7/9 in HEK293 cells, immunoprecipitated and the peptides obtained after tryptic digest were subjected to mass spectrometry analysis. The sequences and theoretical masses of identified peptides are given below the spectra. Methylated peptides were not detected without coexpression of SET7/9 (Figure S7).

enzyme and the target protein domains. The YFP fused target protein domains were purified from the cells by immunoprecipitation and separated by SDS gel electrophoresis. The corresponding gel pieces containing the target protein bands were cut out, the proteins in gel-digested with trypsin and the methylation state of the respective target peptides analyzed by mass spectrometry. It was found that five of the target protein domains (CENPC1, IRF1, MeCP2, MINT, and ZDH8) got methylated inside the human cells when they were coexpressed with SET7/9 but not without coexpression (Figure 4; Figure S7). In case of the four other proteins, we could not detect the peptide containing the target lysine (neither in methylated nor in unmethylated state), and hence we could not determine their methylation status. These results confirm that SET7/9 methylates many of the new targets in vivo.

The MALDI mass spectrometry analysis of MeCP2, IRF1, and MINT revealed that two methyl groups were transferred to the tryptic peptide containing the target lysine, suggesting either dimethylation of the target or monomethylation of two independent lysines (Figure 4). This result agrees with the observation of a second methylation site in the in vitro experiment with MeCP2 and IRF1, which rules out the possibility of dimethylation. The presence of a second methylation site in IRF1 could be explained since it has two KSK motifs nearby. In case of MINT, mutagenesis of the KSK lysine (lysine 2076 of MINT) led to a complete loss of all methylation suggesting that this residue is dimethylated by SET7/9 in cells. Dimethylation of the MINT substrate was confirmed at peptide level as described in the next paragraph.

SET7/9 Product Profile Depends on the Substrate Peptide Sequence

In various studies, the SET7/9 enzyme has been described as a monomethyltransferase (Wang et al., 2001; Xiao et al., 2003; Zhang et al., 2003), and molecular modeling has been applied to explain this product specificity (Guo and Guo, 2007; Zhang and Bruice, 2008). Mutagenesis of Y305F converted the enzyme into a di- and trimethyltransferase (Zhang et al., 2003) leading to

the identification of a similar Tyr/Phe switch in many related enzymes (Collins et al., 2005; Couture et al., 2008; Takahashi et al., 2009; Zhang et al., 2003). As described above, our mass spectrometric analysis of the MINT target provided evidence that dimethylation is introduced into this peptide. To compare the methylation kinetics and product specificity of SET7/9 for the H3 and the MINT peptide, we have synthesized a version of the MINT peptide which contains only one lysine, methylated this peptide together with the H3 peptide in competition in one reaction tube and followed the time course of the reaction by analyzing the products by mass spectrometry at different time points. In this experimental setup and under multiple turnover conditions, the partitioning of the enzyme between the both substrates is determined by the ratio of the K_D-values and turnover is given by k_{cat}. Hence, the relative rates of methylation of both substrates correspond to k_{cat}/K_D, which is a well-established criterion to assess enzyme specificity and activity. We opted for the competitive methylation design because of several advantages: (1) the absolute concentrations of the substrates are not relevant as long as multiple turnover is ensured. (2) Potential pipetting inaccuracies in enzyme and cofactor addition are equally affecting both reactions. (3) Potential synthesis by-products or contaminants affect both reactions equally. However, this design does not allow for direct measurement of the individual K_m and k_{cat} values.

The mass spectrometric analysis revealed that after 6 hours of methylation by SET7/9, only 10% of the H3 peptide was dimethylated, while in case of MINT peptide nearly 50% was dimethylated (Figure 5; Figure S4). However, monomethylated peptides were the main products in the initial time points indicating a nonprocessive reaction mechanism. Fitting to a distributive methylation reaction revealed that the first and second methyl group transfer reactions are about 5-fold faster with the MINT peptide as compared to H3. It is interesting to note that the improved methylation of the MINT peptide was observed even after the K to R exchange at pos. −2, which was necessary for technical reasons to demonstrate dimethylation of one single K residue. According to our results, the original MINT peptide is expected to be an even better substrate. Better methylation of the modified MINT peptide can be attributed to the S residues positioned at −3 and −1, which are both preferred over A and T found in the H3 peptide at the corresponding sites. Most importantly this analysis reveals that the number of methyl groups introduced by the SET7/9 enzyme depends on the sequence of the substrate peptide.

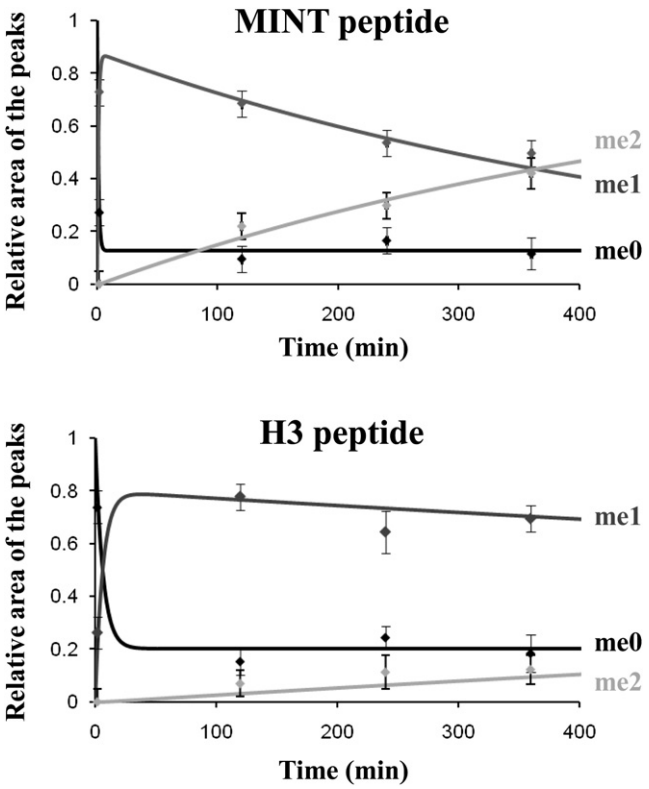

Figure 5. Methylation Kinetics of H3 and a MINT Peptide Variant that Contained Only One Lysine Residue (A N S R S K R G R S R N S A)
H3 peptide and MINT peptide were methylated in competition by SET7/9 and the time course of the reaction by analyzing the products in mass spectrometry at different time points. The relative area of the peaks of the unmethylated (black), monomethylated (dark gray), and dimethylated peptides (light gray) of H3 and MINT were calculated and the data fitted to a distributive two-step methylation process. The fit is shown as solid line (see Figure S4A for primary data). The linear response of the peak area to peptide fractions in the mass spectrometric analyses was confirmed by a calibration experiment (Figure S4B). Error bars were estimated on the basis of two repeats of the experiment and of the results of the calibration experiment.

SET7/9 Activity Is Inhibited by Phosphorylation of the Substrate Peptide or Protein

It is of importance if other modifications influence the activity of SET7/9. On the H3 peptide, it was reported that the SET7/9 activity is reduced by H3K9 trimethylation (Wang et al., 2001) and H3R2 methlyation (Couture et al., 2006). Phosphorylation was shown to inhibit SET7/9 on H3 and the p53 peptide (Couture et al., 2006). In the context of the ER peptide, acetylation of the K at +1 position has been shown to reduce enzyme activity (Subramanian et al., 2008). To study the interference of different modifications on methylation activity of SET7/9, a modified CelluSpot peptide array was methylated by SET7/9 in the presence of radioactively labeled AdoMet (Figure 6A). The array contained 216 peptides derived from the N-terminal tail of H3 featuring 18 different PTMs in many combinations. Among the H3 peptides, we observed the SET7/9 methylation activity was inhibited by H3K4me1, H3K4me2, H3K4me3, and H3K4 acetylation, which confirms the earlier findings that SET7/9 is a monomethyltransferase on the H3 substrate (Figure 4A; Table S2) (Wang et al., 2001; Xiao et al., 2003). We did not observe an inhibition of SET7/9 activity by H3K9 trimethylation, which is in agreement with the finding that K9 is not contacted by the enzyme in the crystal structure (Xiao et al., 2003). We also observed that symmetric or asymmetric methylation of R2 of the H3 tail has no influence on SET7/9 activity (Figure 4A), which is in agreement with the weak contact to R2 observed in the structure. However, phosphorylation of T3, S10, or T11 on the H3 tail abolished the SET7/9 activity completely, which is in line with the general preference of SET7/9 for positively charged substrates mentioned before. Similarly, S14 phosphorylation of H2B (next to the main target K15) inhibited the methylation

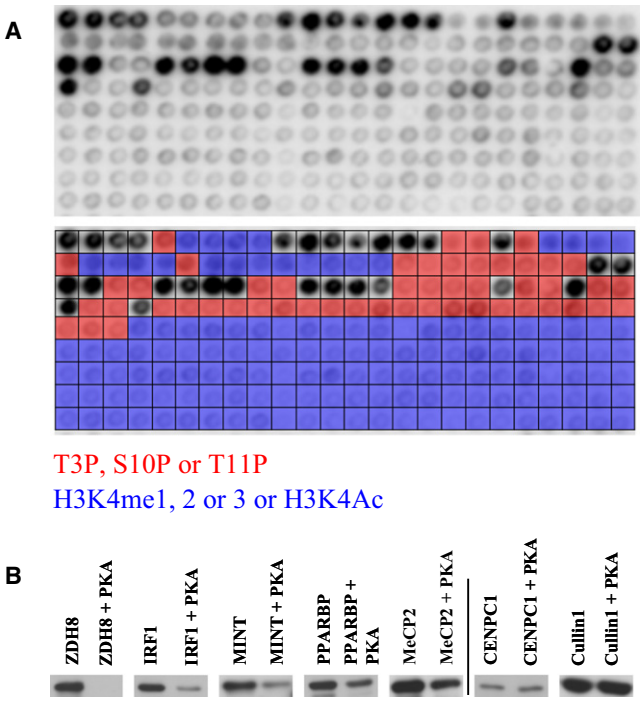

Figure 6. SET7/9 Is Inhibited by Phosphorylation of the Target Peptide or Protein

(A) Relative activity of SET7/9 on CelluSpot array derived from H3 peptides containing different combinations of PTMs (Table S2). Phosphorylation of T3, S10, and T11 abolished SET7/9 activity.

(B) Influence of phosphorylation of nonhistone substrates on SET7/9 methylation activity. GST-tagged nonhistone substrates of SET7/9 were incubated with PKA. All domains except Cullin1 were phosphorylated (Figure S5). Then, phosphorylated and mock treated domains were methylated by SET7/9. A complete loss or strong reduction of SET7/9 activity was observed with ZDN8, IRF1, MINT, PPARBP, and MeCP2.

See also Figure S6.

activity of SET7/9 which underscores the general inhibitory effect of substrate phosphorylation on SET7/9 (Figure 3A).

To investigate the effect of the phosphorylation of nonhistone proteins on SET7/9 activity, we used GPS2.0 (Xue et al., 2008) to predict kinases that could act on the protein domains. This analysis revealed that most of the nonhistone protein domains are potential substrates for several major kinases including protein kinase A (PKA). Therefore, we incubated the GST-tagged nonhistone substrates with PKA and observed clear phosphorylation of all domains except Cullin1 (Figure S5). The phosphorylated and mock treated domains were methylated by SET7/9 revealing a complete loss or strong reduction of SET7/9 activity after phosphorylation of ZDN8, IRF1, MINT, PPARBP, and MeCP2 (Figure 6B). We investigated the target protein domains isolated from HEK293 cells after coexpression of the SET7/9 enzyme and the target protein domains for potential phosphorylation next to the target lysine by mass spectrometry. Phosphorylation within the tryptic peptides that contain the target lysine was observed for IRF1 and MINT (Figure S5). However, we could not detect target peptides containing both the methylation and phosphorylation marks suggesting that phosphorylation inhibits SET7/9 methylation in vivo as well. These results indicate that the SET7/9 signaling pathway is tightly connected to protein phosphorylation.

DISCUSSION

Peptide arrays are ideal tools to investigate the specificity of PKMTs, because they allow determining the enzymatic activity for more than 400 different substrates in a single experiment in competition. It is also possible to design partially randomized arrays of peptides based on an initial sequence motif to find unpredicted new substrate specificities. The peptide array-based approach was successfully used in our lab previously to identify new targets for G9a and to study the specificity of Dim5 (Rathert et al., 2008a, 2008b). In the present study, we discovered an optimized target sequence motif for SET7/9 in a series of peptide array methylation experiments in total including more than 1200 different peptides. Based on our specificity profile, we identified 91 new target peptides, about one-third of which were better substrates for SET7/9 than the originally described histone 3 target. We confirmed methylation of selected strongly methylated candidate peptides at the protein domain level in vitro and in vivo with a high success rate suggesting that there are many more methylation substrates of SET7/9 are among our list of peptide substrates. Altogether, we show methylation of nine nonhistone proteins plus methylation of H2A and H2B, which more than doubles the number of known SET7/9 targets. Methylation of H2A and B had not been observed with histone octamers (Wang et al., 2001), suggesting that only free H2A and B are substrates for SET7/9. This situation is comparable with NSD2, which methylates the free H4 protein but not in the context of nucleosomes (Li et al., 2009). It is known that a fraction of histone H3 and H4 carry some modifications prior to their incorporation into chromatin (Barth and Imhof, 2010). Whether methylation of free H2A and H2B histone proteins by SET7/9 occurs and if it has a physiological role remains to be seen.

A comparison of known and novel SET7/9 substrates (Figure 2D) with the combined specificity profile [GRHKPST] [K > R] [S > KYARTPN] K [QN] [AQGMSPTYV] indicates that all targets follow the profile at the −1 and −2 positions (Figure 2D). Position −3 also applies often, while the +1 and +2 positions appear less important suggesting that a [GRHKPST] [K > R] [S > KYARTPN] K motif will be most appropriate to search for additional SET7/9 substrates. It is important to note that peptides not ideally matching this sequence (like some of the previously known SET7/9 targets) can be methylated as well, although methylation often is weaker at peptide level (see, for example, Dnmt1, ER, Tat, or p65 in Figure 2A). Additional target Set7/9 sites were identified that do not follow the consensus, including NF-kappaB p65 K314 and K315 (Yang et al., 2009), Rb K873 (Munro et al., 2010), and several methylation sites in PCAF (Masatsugu and Yamamoto, 2009). However, these sites were all methylated with lower efficiency than H3K4, while strong targets identified here, which follow the consensus, all are methylated better than H3K4. Weaker methylation does not rule out important biological roles of these methylation events, because in the cell a strong interaction of a target protein with the SET7/9 enzyme may stimulate methylation of weak target sites.

We have shown that the SET7/9 activity on histone tails and nonhistone substrates is inhibited by serine phosphorylation

indicating a general crosstalk between phosphorylation and SET7/9 mediated methylation of histone and nonhistone proteins as previously shown for E2F1 (Kontaki and Talianidis, 2010). Monomethylation of lysine directly blocks its acetylation, but it may also influence acetylation of remote sites in a more complex manner. SET7/9 methylation is necessary for it subsequent acetylation by Tip60 (Ivanov et al., 2007; Kurash et al., 2008), but it inhibits acetylation of E2F1 (Kontaki and Talianidis, 2010). In cells, SET7/9 methylation has been shown to increase stability of p53 (Chuikov et al., 2004) but decrease Dnmt1 stability (Esteve et al., 2009; Wang et al., 2009).

SIGNIFICANCE

SET7/9 (KMT7) is a protein lysine methyltransferase (PKMT) that had been initially identified as a histone H3 lysine-4 monomethyltransferase, but nonhistone substrates of this enzyme were discovered later. In the present study we apply peptide array methylation to determine an optimized target sequence motif for SET7/9 as [GRHKPST] [K > R] [S > KYA RTPN] K (with the target lysine underlined) surrounded by basic amino acid residues. Based on this, we discover 91 new peptide SET7/9 substrates and show methylation of nine nonhistone proteins (AKA6, CENPC1, MeCP2, MINT, PPARBP, ZDH8, Cullin1, IRF1, and [weakly] TTK) plus methylation of H2A and H2B, which more than doubles the number of known SET7/9 targets. Our results contribute to the emerging picture that lysine methylation is a widespread posttranslational modification. Our data document that novel PKMT substrates, which are methylated better than previously known substrates, can be identified following an unbiased approach. We show that SET7/9 is inhibited by phosphorylation of histone and nonhistone substrate proteins indicating that nonhistone protein methylation by SET7/9 is connected to other signaling pathways like phosphorylation and acetylation. Finally, we show that one lysine residue in the MINT protein is dimethylated by SET7/9 in vitro and in vivo demonstrating that the product spectrum of PKMTs depends on the nature of the substrate. This finding adds another level of complexity to the function of PKMTs.

EXPERIMENTAL PROCEDURES

Cloning, Expression, and Purification of Proteins

The sequence encoding human A kinase anchor protein 6 (AKA6) (residues 485–776; NCBI accession number NP_004265.3), Bromodomain containing 1 (BRD1) (residues 681–891; NCBI accession number NP_055392.1), Centromeric protein C1 (CENPC1) (residues 279–474; NCBI accession number NP_001803.2), Dnmt1 (residues 622–780; NCBI accession number NP_001370.1), Methyl CpG binding protein 2 (MeCP2) (residues 201–486; NCBI accession number NP_004983.1), Msx2-interacting protein (MINT) (residues 1994–2281; NCBI accession number NP_055816.2), PPAR binding protein (PPARBP) (residues 847–1084; NCBI accession number NP_004765.2), Retinoblastoma binding protein 5 (RBBP5) (residues 323–538; NCBI accession number NP_005048.2), Zinc finger DHHC domain containing 8 (ZDHHC8) (residues 227–400; NCBI accession number NP_037505.1), PRP4 pre-mRNA processing factor 4 homolog B (PRP4) (residues 93–396; NCBI accession number NP_789770.1) CDC2 related protein kinase 7 (CRKRS) (residues 2–339; NCBI accession number NP_057591.1), Cullin1 (residues 2–250; NCBI accession number NP_003583.2), TTK (residues 603–799; NCBI accession number NP_003309.2), and IRF1 (residues 71–240; NCBI accession number NP_002189.1) were amplified from HEK293 cDNA and cloned into pENTR/D-TOPO (Invitrogen) gateway entry vector according to the manufacturer's instructions. pGEX-6P-2 vector (GE healthcare) was converted into Gateway destination vector (pGEX-6P-2-GW-AJ) using Gateway vector conversion system (Invitrogen). The cloned genes from the pENTR/D-TOPO were subcloned into pGEX-6P-2-GW-AJ using LR recombination system (Invitrogen) according to the manufacturer's instructions.

For mammalian expression, an oligonucleotide coding for the nuclear localization signal of simian virus large T-antigen was cloned in frame with YFP protein in pEYFP-C1 vector (Clontech) by using BspEI/XhoI sites to generate the pEYFP-C1-AJ-NLS construct. The target protein domains were subcloned into pEYFP-C1-AJ-NLS by using XhoI/EcoRI sites except AKA6. The protein domain of AKA6 was subcloned into pEYFP-C1-AJ-NLS by using XhoI/BamHI site. The full-length SET7/9 enzyme was subcloned into pCDNA4/myc-His vector (Invitrogen) using BamHI/XhoI sites.

The K604R mutation in AKA6, K414R mutation in CENPC1, K347R mutation in MeCP2, K2076R mutation in MINT, K1006R mutation in PPARBP, K300R mutation in ZDH8, K73R mutation in Cullin1, K708R mutation in TTK, and K126R mutation in IRF1 were introduced using PCR-megaprimer mutagenesis method as previously described (Jeltsch and Lanio, 2002). Mutagenesis was confirmed by restriction marker site analysis and DNA sequencing.

For expression, *Escherichia coli* BL21 (Novagen) carrying corresponding plasmid were grown in Luria-Bertani medium at 37°C to OD_{600} ≈0.6, then shifted to 22°C for 20 min and induced overnight with 1 mM isopropyl β-D-thiogalactoside. The cells were collected by centrifugation and resuspended in 20 mM HEPES (pH 7.5), 0.5 M KCl, 0.2 mM DTT, 1 mM EDTA, and 10% glycerol and disrupted by sonication. The supernatants were passed through glutathione Sepharose 4B resin (Amersham Biosciences) and washed with same buffer. The bound proteins were eluted with similar buffer containing 40 mM glutathione and dialyzed in 20 mM HEPES (pH 7.5), 0.2 M KCl, 0.2 mM DTT, 1 mM EDTA, and 10% glycerol for 2 hr and then overnight in 20 mM HEPES (pH 7.5), 0.2 M KCl, 0.2 mM DTT, 1 mM EDTA, and 60% glycerol. The SET7/9 expression construct pXC367 was kindly provided by Prof. Xiodong Cheng. The SET7/9 enzyme was expressed and purified as described (Zhang et al., 2003). Recombinant histone 3 (3.1), histone H2A, and histone H2B were purchased from New England Biolabs.

Synthesis of Peptide SPOT Arrays

Peptide arrays were synthesized using the SPOT synthesis method (Frank, 2002; Wenschuh et al., 2000). Each spot had a diameter of 2 mm and contained approximately 9 nmol of peptide (Autospot Reference Handbook, Intavis AG). Successful synthesis of each peptide was confirmed by bromphenol blue staining of the membranes after each cycle. The CelluSpot glass slide histone tail peptide array was purchased from Intavis AG, Germany.

Solid-Phase Peptide Synthesis

A variant of the MINT peptide containing only one lysine residue (A N S R S K R G R S R N S A) was synthesized by following the Fmoc solid-phase peptide synthesis and the synthesis was confirmed by mass spectrometry. The sequence of the MINT peptide was modified to contain single target lysine in order to follow the degree of methylation at the target lysine. Biotinylated histone 3 peptide (residues 1–20) was purchased from JPT Peptide Technologies.

Methylation of Peptide Arrays

The membranes containing 420 peptide spots were washed for 20 min in methylation buffer containing 50 mM Tris/HCl (pH 9.0), 5 mM $MgCl_2$, and 4 mM DTT and afterward incubated at ambient temperature for 45 min in methylation buffer containing 20 nM SET7/9 enzyme and 0.76 μM labeled [methyl-3H]-AdoMet (Perkin Elmer). The membranes were washed four times with 50 mM NH_4HCO_3, dried between Whatman papers (Whatman GmbH, Dassel, Germany), and rinsed with Amplify NAMP100V solution (GE Healthcare, Munich, Germany). The membranes were incubated on HyperfilmTM high performance autoradiography films (GE Healthcare, Munich, Germany) in the dark for 3–7 days. The films were developed using AGFA Curix 60 developing machine (Agfa Deutschland Vertriebsgesellschaft mbH & Co. KG, Cologne, Germany) and the radioactive incorporation quantified using

Phoretix Software. Methylation of CelluSpot glass slide array was performed in a similar way as described above.

In Vitro Methylation of Protein Domains

Protein domain methylation reactions were performed in methylation buffer (50 mM Tris/HCl [pH 9.0], 5 mM $MgCl_2$, 4 mM DTT) supplemented with 0.76 μM tritium-labeled AdoMet (specific activity: 2.7 TBq/mmol; Perkin Elmer). Target proteins (2 μM) were incubated with 100 nM SET7/9 for overnight at 37°C. An aliquot of 10 μl of the reaction mixtures were loaded on 12% SDS PAGE and separated and the amount of methylation was detected by autoradiography.

Competitive Methylation of H3 and MINT Peptides

Two hundred nanomolar of biotinylated histone 3 (1-20) peptide and MINT peptide variant containing only a single lysine residue were subjected to competitive methylation in one reaction mixture with 10 nM SET7/9 enzyme in methylation buffer (50 mM Tris/HCl [pH 9.0], 5 mM $MgCl_2$, 4 mM DTT, and 200 μM AdoMet). The reaction was carried out at room temperature and samples were collected from the reaction vial at different time points to check the conversion of substrate peptides to mono- and dimethylated products. The methylation status of the peptides was analyzed by mass spectrometry.

In Vitro Phosphorylation of Protein Domains

Protein domains (2 μM) were phosphorylated with 1000 units of cAMP-dependent Protein Kinase (PKA) catalytic subunit (NEB, P6000S) for 2 hr at 30°C in 50 mM Tris (pH 7.5), 10 mM $MgCl_2$ supplemented with 123 nM [γ-32P]-ATP (specific activity 30 TBq/mmol; Hartmann Analytic GmbH). An aliquot of 20 μl of the reaction mixtures was loaded on 12% SDS PAGE and separated and the amount of phosphorylation was detected by Phosphor Imager.

To study the interference of substrate protein phosphorylation on the methylation activity of SET7/9, the target proteins were phosphorylated in the presence of unlabeled ATP (200 μM final concentration) as described above. Afterward, the phosphorylated proteins were methylated using 100 nM SET7/9 in the presence of 0.76 μM tritium-labeled AdoMet for 2 hr at 37°C. An aliquot of 10 μl of the reaction mixtures was loaded on 12% SDS PAGE, separated and the amount of methylation was detected by autoradiography.

Cell Culture, Transfection, and Immunoprecipitation

The target protein domain constructs were transfected together with SET7/9 expression construct or without SET7/9 expression construct in HEK293 cells using the transfection reagent FuGene6 (Roche) according to the manufacturer's instructions. Two days after transfection, the nuclear extracts were prepared as described (Andrews and Jones, 1991). Immunoprecipitation of target protein domains in the nuclear extracts was performed by using Living Colors Full-Length A.v. Polyclonal Antibody (Clontech) and Dynabeads Protein G (Invitrogen) according to the manufacturers' instructions.

Mass Spectrometry Analysis

The immunoprecipitated target protein domains were separated on 12% SDS-PAGE and the bands of expected size were excised and further processed for MALDI mass spectrometric analysis using an Autoflex II device (Bruker Daltonics) as described (Shevchenko et al., 2006). After overnight in gel digestion of the target protein with 1 μg of Trypsin Gold (Promega) in a reaction volume of 50 μl, the peptides samples were diluted 1:5 with 0.1% TFA and subjected to MALDI analysis as described below. In case of competitive methylation of H3 and MINT peptides, 1 μl of the reaction mixtures were diluted 1:10 in 0.1% TFA and subjected to MALDI analysis as described below.

One microliter of the peptide dilution was applied to one spot on a prespotted Anchorchip (PAC) HCCA Plate (Cat. No. 227463, Bruker Daltonics) and washed with 10 mM sodium phosphate / 0.1% TFA solution. Spectra were recorded using an AutoFlex II (Bruker Daltonics, Bremen, Germany) with default settings using peptide calibration standard mixture with the mass range of 1000 to 4000 Da (Cat. No. 206195, Bruker Daltonics) and processed using the FlexAnalysis software (Bruker Daltonics). Protein methylation and phosphorylation was investigated using the Biotools program (Bruker Daltonics). Methylated peptide peaks were not observed in protein domains purified from *E. coli*. The corresponding masses could not be matched to any unmodified full or partially digested peptide from the target proteins.

SUPPLEMENTAL INFORMATION

Supplemental Information includes seven figures and four tables and can be found with this article online at doi:10.1016/j.chembiol.2010.11.014.

ACKNOWLEDGMENTS

This work was partially supported by the DFG JE 252/7 and NIH DK08267 grants. We gratefully acknowledge gift of a SET7/9 expression construct by Prof. Xiaodong Cheng.

Received: August 9, 2010
Revised: November 17, 2010
Accepted: November 18, 2010
Published: January 27, 2011

REFERENCES

Andrews, P.A., and Jones, J.A. (1991). Characterization of binding proteins from ovarian carcinoma and kidney tubule cells that are specific for cisplatin modified DNA. Cancer Commun. *3*, 93–102.

Barth, T.K., and Imhof, A. (2010). Fast signals and slow marks: the dynamics of histone modifications. Trends Biochem. Sci. *35*, 618–626.

Brasacchio, D., Okabe, J., Tikellis, C., Balcerczyk, A., George, P., Baker, E.K., Calkin, A.C., Brownlee, M., Cooper, M.E., and El-Osta, A. (2009). Hyperglycemia induces a dynamic cooperativity of histone methylase and demethylase enzymes associated with gene-activating epigenetic marks that coexist on the lysine tail. Diabetes *58*, 1229–1236.

Chakrabarti, S.K., Francis, J., Ziesmann, S.M., Garmey, J.C., and Mirmira, R.G. (2003). Covalent histone modifications underlie the developmental regulation of insulin gene transcription in pancreatic beta cells. J. Biol. Chem. *278*, 23617–23623.

Chuikov, S., Kurash, J.K., Wilson, J.R., Xiao, B., Justin, N., Ivanov, G.S., McKinney, K., Tempst, P., Prives, C., Gamblin, S.J., et al. (2004). Regulation of p53 activity through lysine methylation. Nature *432*, 353–360.

Collins, R.E., Tachibana, M., Tamaru, H., Smith, K.M., Jia, D., Zhang, X., Selker, E.U., Shinkai, Y., and Cheng, X. (2005). In vitro and in vivo analyses of a Phe/Tyr switch controlling product specificity of histone lysine methyltransferases. J. Biol. Chem. *280*, 5563–5570.

Couture, J.F., Collazo, E., Hauk, G., and Trievel, R.C. (2006). Structural basis for the methylation site specificity of SET7/9. Nat. Struct. Mol. Biol. *13*, 140–146.

Couture, J.F., Dirk, L.M., Brunzelle, J.S., Houtz, R.L., and Trievel, R.C. (2008). Structural origins for the product specificity of SET domain protein methyltransferases. Proc. Natl. Acad. Sci. USA *105*, 20659–20664.

Deering, T.G., Ogihara, T., Trace, A.P., Maier, B., and Mirmira, R.G. (2009). Methyltransferase Set7/9 maintains transcription and euchromatin structure at islet-enriched genes. Diabetes *58*, 185–193.

Ea, C.K., and Baltimore, D. (2009). Regulation of NF-kappaB activity through lysine monomethylation of p65. Proc. Natl. Acad. Sci. USA *106*, 18972–18977.

Esteve, P.O., Chin, H.G., Benner, J., Feehery, G.R., Samaranayake, M., Horwitz, G.A., Jacobsen, S.E., and Pradhan, S. (2009). Regulation of DNMT1 stability through SET7-mediated lysine methylation in mammalian cells. Proc. Natl. Acad. Sci. USA *106*, 5076–5081.

Evans-Molina, C., Robbins, R.D., Kono, T., Tersey, S.A., Vestermark, G.L., Nunemaker, C.S., Garmey, J.C., Deering, T.G., Keller, S.R., Maier, B., et al. (2009). Peroxisome proliferator-activated receptor gamma activation restores islet function in diabetic mice through reduction of endoplasmic reticulum stress and maintenance of euchromatin structure. Mol. Cell. Biol. *29*, 2053–2067.

Frank, R. (2002). The SPOT-synthesis technique. Synthetic peptide arrays on membrane supports–principles and applications. J. Immunol. Methods *267*, 13–26.

Guo, H.B., and Guo, H. (2007). Mechanism of histone methylation catalyzed by protein lysine methyltransferase SET7/9 and origin of product specificity. Proc. Natl. Acad. Sci. USA *104*, 8797–8802.

Ivanov, G.S., Ivanova, T., Kurash, J., Ivanov, A., Chuikov, S., Gizatullin, F., Herrera-Medina, E.M., Rauscher, F., 3rd, Reinberg, D., and Barlev, N.A. (2007). Methylation-acetylation interplay activates p53 in response to DNA damage. Mol. Cell. Biol. *27*, 6756–6769.

Jeltsch, A., and Lanio, T. (2002). Site-directed mutagenesis by polymerase chain reaction. Methods Mol. Biol. *182*, 85–94.

Kontaki, H., and Talianidis, I. (2010). Lysine methylation regulates E2F1-induced cell death. Mol. Cell *39*, 152–160.

Kouskouti, A., Scheer, E., Staub, A., Tora, L., and Talianidis, I. (2004). Gene-specific modulation of TAF10 function by SET9-mediated methylation. Mol. Cell *14*, 175–182.

Kurash, J.K., Lei, H., Shen, Q., Marston, W.L., Granda, B.W., Fan, H., Wall, D., Li, E., and Gaudet, F. (2008). Methylation of p53 by Set7/9 mediates p53 acetylation and activity in vivo. Mol. Cell *29*, 392–400.

Li, Y., Trojer, P., Xu, C.F., Cheung, P., Kuo, A., Drury, W.J., 3rd, Qiao, Q., Neubert, T.A., Xu, R.M., Gozani, O., et al. (2009). The target of the NSD family of histone lysine methyltransferases depends on the nature of the substrate. J. Biol. Chem. *284*, 34283–34295.

Masatsugu, T., and Yamamoto, K. (2009). Multiple lysine methylation of PCAF by Set9 methyltransferase. Biochem. Biophys. Res. Commun. *381*, 22–26.

Munro, S., Khaire, N., Inche, A., Carr, S., and La Thangue, N.B. (2010). Lysine methylation regulates the pRb tumour suppressor protein. Oncogene *29*, 2357–2367.

Pagans, S., Kauder, S.E., Kaehlcke, K., Sakane, N., Schroeder, S., Dormeyer, W., Trievel, R.C., Verdin, E., Schnolzer, M., and Ott, M. (2010). The Cellular lysine methyltransferase Set7/9-KMT7 binds HIV-1 TAR RNA, monomethylates the viral transactivator Tat, and enhances HIV transcription. Cell Host Microbe *7*, 234–244.

Rathert, P., Dhayalan, A., Murakami, M., Zhang, X., Tamas, R., Jurkowska, R., Komatsu, Y., Shinkai, Y., Cheng, X., and Jeltsch, A. (2008a). Protein lysine methyltransferase G9a acts on non-histone targets. Nat. Chem. Biol. *4*, 344–346.

Rathert, P., Zhang, X., Freund, C., Cheng, X., and Jeltsch, A. (2008b). Analysis of the substrate specificity of the Dim-5 histone lysine methyltransferase using peptide arrays. Chem. Biol. *15*, 5–11.

Reineke, U., Volkmer-Engert, R., and Schneider-Mergener, J. (2001). Applications of peptide arrays prepared by the SPOT-technology. Curr. Opin. Biotechnol. *12*, 59–64.

Shevchenko, A., Tomas, H., Havlis, J., Olsen, J.V., and Mann, M. (2006). In-gel digestion for mass spectrometric characterization of proteins and proteomes. Nat. Protoc. *1*, 2856–2860.

Subramanian, K., Jia, D., Kapoor-Vazirani, P., Powell, D.R., Collins, R.E., Sharma, D., Peng, J., Cheng, X., and Vertino, P.M. (2008). Regulation of estrogen receptor alpha by the SET7 lysine methyltransferase. Mol. Cell *30*, 336–347.

Takahashi, Y.H., Lee, J.S., Swanson, S.K., Saraf, A., Florens, L., Washburn, M.P., Trievel, R.C., and Shilatifard, A. (2009). Regulation of H3K4 trimethylation via Cps40 (Spp1) of COMPASS is monoubiquitination independent: implication for a Phe/Tyr switch by the catalytic domain of Set1. Mol. Cell. Biol. *29*, 3478–3486.

Wang, H., Cao, R., Xia, L., Erdjument-Bromage, H., Borchers, C., Tempst, P., and Zhang, Y. (2001). Purification and functional characterization of a histone H3-lysine 4-specific methyltransferase. Mol. Cell *8*, 1207–1217.

Wang, J., Hevi, S., Kurash, J.K., Lei, H., Gay, F., Bajko, J., Su, H., Sun, W., Chang, H., Xu, G., et al. (2009). The lysine demethylase LSD1 (KDM1) is required for maintenance of global DNA methylation. Nat. Genet. *41*, 125–129.

Weiss, T., Hergeth, S., Zeissler, U., Izzo, A., Tropberger, P., Zee, B.M., Dundr, M., Garcia, B.A., Daujat, S., and Schneider, R. (2010). Histone H1 variant-specific lysine methylation by G9a/KMT1C and Glp1/KMT1D. Epigenetics Chromatin *3*, 7.

Wenschuh, H., Volkmer-Engert, R., Schmidt, M., Schulz, M., Schneider-Mergener, J., and Reineke, U. (2000). Coherent membrane supports for parallel microsynthesis and screening of bioactive peptides. Biopolymers *55*, 188–206.

Xiao, B., Jing, C., Wilson, J.R., Walker, P.A., Vasisht, N., Kelly, G., Howell, S., Taylor, I.A., Blackburn, G.M., and Gamblin, S.J. (2003). Structure and catalytic mechanism of the human histone methyltransferase SET7/9. Nature *421*, 652–656.

Xue, Y., Ren, J., Gao, X., Jin, C., Wen, L., and Yao, X. (2008). GPS 2.0, a tool to predict kinase-specific phosphorylation sites in hierarchy. Mol. Cell. Proteomics *7*, 1598–1608.

Yang, X.D., Huang, B., Li, M., Lamb, A., Kelleher, N.L., and Chen, L.F. (2009). Negative regulation of NF-kappaB action by Set9-mediated lysine methylation of the RelA subunit. EMBO J. *28*, 1055–1066.

Zhang, X., and Bruice, T.C. (2008). Enzymatic mechanism and product specificity of SET-domain protein lysine methyltransferases. Proc. Natl. Acad. Sci. USA *105*, 5728–5732.

Zhang, X., Yang, Z., Khan, S.I., Horton, J.R., Tamaru, H., Selker, E.U., and Cheng, X. (2003). Structural basis for the product specificity of histone lysine methyltransferases. Mol. Cell *12*, 177–185.

